



Journal of Applied Science

Biannual Peer Reviewed Journal Issued by Research and Consultation Center , Sabratha University

Issue (13)
September 2024





Journal of Applied Science

Biannual Peer Reviewed Journal Issued by Research and Consultation Center,
Sabratha University

Editor

Dr. Hassan M. Abdalla

Associate Editors

Dr. Elsaïd M. Shwaia

Dr. Elsaïd A. Elajoz (Egypt)

Dr. Antonio M. Camposs (Portugal)

Dr. Jbireal M. Jbireal

Dr. Salma F. Naji

Dr. Ahmed F. Elsgair (Egypt)

English Language Reviewer

Dr. Siham S. Abdelrahman

Arabic Language Reviewer

Dr. Ebrahim K. Altwade

Designed By

Anesa M. Al-najeh

Editorial

We start this pioneering work, which do not seek perfection as much as aiming to provide a scientific window that opens a wide area for all the distinctive pens, both in the University of Sabratha or in other universities and research centers. This emerging scientific journal seeks to be a strong link to publish and disseminate the contributions of researchers and specialists in the fields of applied science from the results of their scientific research, to find their way to every interested reader, to share ideas, and to refine the hidden scientific talent, which is rich in educational institutions. No wonder that science is found only to be disseminated, to be heard, to be understood clearly in every time and place, and to extend the benefits of its applications to all, which is the main role of the University and its scholars and specialists. In this regard, the idea of issuing this scientific journal was the publication of the results of scientific research in the fields of applied science from medicine, engineering and basic sciences, and to be another building block of Sabratha University, which is distinguished among its peers from the old universities.

As the first issue of this journal, which is marked by the Journal of Applied Science, the editorial board considered it to be distinguished in content, format, text and appearance, in a manner worthy of all the level of its distinguished authors and readers.

In conclusion, we would like to thank all those who contributed to bring out this effort to the public. Those who lit a candle in the way of science which is paved by humans since the dawn of creation with their ambitions, sacrifices and struggle in order to reach the truth transmitted by God in the universe. Hence, no other means for the humankind to reach any goals except through research, inquiry, reasoning and comparison.

Editorial Committee

Notice

The articles published in this journal reflect the opinions of their authors only. They are solely bearing the legal and moral responsibility for their ideas and opinions. The journal is not held responsible for any of that.

Publications are arranged according to technical considerations, which do not reflect the value of such articles or the level of their authors.


Journal Address:

Center for Research and Consultations, Sabratha University

Website: <https://jas.sabu.edu.ly/index.php/asjsu>

Email: jas@sabu.edu.ly

Local Registration No. (435/2018)

ISSN  2708-7301

ISSN  2708-7298

Publication instructions

The journal publishes high quality original researches in the fields of Pure Science, Engineering and Medicine. The papers can be submitted in English or Arabic language through the Journal email (jas@sabu.edu.ly) or CD. The article field should be specified and should not exceed 15 pages in single column.

All submitted research manuscripts must follow the following pattern:

- Title, max. 120 characters.
- Author Name, Affiliation and Email
- Abstract, max. 200 words.
- Keywords, max. 5 words.
- Introduction.
- Methodology.
- Results and Discussion.
- Conclusion.
- Acknowledgments (optional).
- References.

Writing Instructions:

Papers are to be submitted in A4 (200×285 mm) with margins of 25 mm all sides except the left side, which should be 30 mm. Line spacing, should also be 1.15.

Table 1. Font size and style

	Bold	English	Arabic
Font Style	✓	Times New Roman	Simplified Arabic
Article Title	✓	14 Capital	16
Authors Name	✓	12	14
Affiliation	×	11	13
Titles	✓	12	14
Sub-Title	✓	12	13
Text	×	12	14
Figure Title	✓	11	13
Table Title	✓	11	13
Equations	✓	12	14

Figures:

All figures should be compatible with Microsoft Word with serial numerals. Leave a space between figures or tables and text.

References:

The references should be cited as Harvard method, eg. Smith, R. (2006). References should be listed as follows:

Articles: Author(s) name, Year, Article Title, Journal Name, Volume and Pages.

Books: Author(s) name. Year. "Book title" Location: publishing company, pp.

Conference Proceedings Articles: Author(s) name. Year. "Article title". Conference proceedings. pp.

Theses: Author(s) name. Year. "Title". Degree level, School and Location.

Invitation

The Editorial Committee invites all researchers "Lecturers, Students, Engineers at Industrial Fields" to submit their research work to be published in the Journal. The main fields targeted by the Journal are:

- Basic Science.
- Medical Science & Technology.
- Engineering.

Refereeing

The Editorial Committee delivers researches to two specialized referees, in case of different opinions of arbitrators the research will be delivered to a third referee.

Editorial Committee

Dr. Hassan M. Abdalla.
Dr. Elsaid M. Shwaia.
Dr. Jbireal M. Jbireal.
Dr. Elsaid A. Elajoz (Egypt).
Dr. Salma F. Naji.
Dr. Antonio M. Camposs (Portugal).
Dr. Ahmed F. Elsgair (Egypt).
Dr. Siham S. Abdelrahman.
Dr. Ebrahim K. Altwade.
Anesa M. Al-najeh.

CONTENTS

[1] EVALUATION OF DOMINO EFFECT CAUSED BY POOL FIRE IN A TANK FARM	1
[2] ASSESSMENT OF HYDRAULIC PARAMETERS OF THE QUATERNARY AQUIFER USING PUMPING TEST, JIFARAH PLAIN, NORTHWEST LIBYA	20
[3] PREVALENCE OF TRICHOMONAS TENAX IN PATIENTS WITH PERIODONTAL DISEASE IN SURMAN CITY	38
[4] SOLUTION OF ABEL’S INTEGRAL EQUATION USING ABAOUB-SHKHEAM TRANSFORM	47
[5] MUSCULOSKELETAL DISORDER AMONG WORKERS IN MISURATA STEEL FACTORY	55
[6] AFFECTION OF MOORE–PENROSE GENERALIZED INVERSE ON MATRICES OF CUBIC COMPLETE GRAPH AND NON-EMPTY REGULAR (COMPLETE) GRAPH	63
[7] PINCH ANALYSIS OF HEAT INTEGRATION AND HEAT EXCHANGER NETWORK DESIGN WITH ASPEN ENERGY ANALYZER IN A NATURAL GAS SWEETENING UNIT	73
[8] ASSESSMENTS OF RADIOACTIVITY CONCENTRATION LEVELS FOR NATURAL RADIONUCLIDES IN SOIL SAMPLES FROM ZLITEN	84
[9] ELECTROCHEMICAL TECHNOLOGIES FOR HYDROGEN PRODUCTION: A REVIEW	94
[10] SIMPLIFIED SUPERSTRUCTURE APPROACH FOR DESIGNING HEAT EXCHANGER NETWORK IN HEATING SYSTEMS OF DISTILLATION CRUDE OIL UNIT: ZAWIYA REFINERY PLANT CASE STUDY	109
[11] 3.5 GHZ BANDWIDTH AND PATTERN RECONFIGURABLE ANTENN	128

3.5 GHZ BANDWIDTH AND PATTERN RECONFIGURABLE ANTENNA

Abdurazag Khalat

Department of Electrical Engineering, Sabratha University, Libya

A.Khalat@sabu.edu.ly

Abstract

This paper presents a reconfigurable antenna (RA) capable of varying its impedance bandwidth between 3.4–3.6 GHz and 3.1–3.9 GHz frequency bands and steering its main beam into three different directions corresponding to $\theta \in \{-30^\circ, 0^\circ, 30^\circ\}$, $\varphi \in \{0^\circ\}$ for each band. The RA employs a multilayer structure, where two parasitically coupled reconfigurable layers, using PIN diode switches, enable the generation of the modes of operation. A fully functional RA has been fabricated and characterized. The characterizations involved measurements of impedance, radiation patterns, error vector magnitude (EVM), and intermodulation (IM). An average realized gain of 9 dB has been achieved for all modes of operation. EVM measurements indicate less than -25 dB EVM for input powers up to 30 dBm. IM test results revealed that passive factors, such as loose solder joints and electrothermal effects, are the main contributors to passive IM products.

Keywords: Aperture coupling; Reconfigurable antennas; Microstrip antennas; Multifrequency antennas; Frequency control.

Introduction

“Spectrum sharing has gained significant attention in recent years due to the scarcity of available spectrum at lower frequency bands and the underutilization of licensed bands” (Ge, L. & Luk, K.M., 2016). The goal is to enable secondary or tertiary users or devices to access the unused licensed spectrum, provided that the primary users of the licensed bands are not harmfully interfered Goldsmith, (A, Jafar, S.A., Maric, I. & Srinivasa, S., 2009). In general, wideband sensing capability is required to determine the available bands where transmission is permitted. To that end, a wideband antenna for sensing the spectrum and a reconfigurable narrowband antenna (RA) with frequency tunability enabling communication on the available bands are needed. Typically, two separate antennas—a large-size wideband antenna and a small-size reconfigurable narrowband antenna—are integrated on the same platform (Erfani, E., Nourinia, J., Ghobadi, C., Niroo-Jazi, M. & Denidni, T.A., 2012).

While this technique offers both wideband and narrowband operations, poor isolation between sensing and communication antennas due to limited available space can

degrade system-level performance. Therefore, a single RA with bandwidth reconfigurable properties that can be used for both sensing and communication to improve isolation between sensing and communication would be advantageous (Cetiner, B., Jafarkhani, H., Qian, J.-Y., Yoo, H.J., Grau, A. & De Fla-Viis, F., 2004).

The single RA element presented in this work is capable of performing both wide and narrow bandwidth operations. In addition, this RA can steer its main radiation beam towards three different directions for both bands. Combining bandwidth and pattern reconfigurability in a single compact platform provides advantages in effective sensing, transmission, and frequency reuse. This RA design consists of a four-layer structure with three reconfigurable layers and a driven antenna layer. Radiation and impedance properties, i.e., reflection coefficient and radiation pattern, are most commonly used to characterize antennas. As the goal of using RAs in a transceiver system is to benefit the overall system-level performance, characterization of the impacts that an RA has on parameters such as Error Vector Magnitude (EVM)—used to quantify the performance of a transceiver—becomes important. Also, signal distortion due to intermodulation (IM) products, whether passive IM (PIM) or due to active elements such as PIN diodes, needs to be measured to properly represent the full impact of antenna characteristics on system performance. Signal distortion measurements have traditionally focused on the RF frontend (RFFE). However, tighter integration between the RFFE and antennas and the increased use of various nonlinear devices, such as PIN and varactor diodes, in antenna terminals makes the system vulnerable to nonlinear distortions. Therefore, it is necessary to measure and minimize these distortions in antenna terminals to ensure high performance. For traditional non-reconfigurable antennas, some works have investigated EVM and passive intermodulation (PIM) (Tawk, Y. & Christodoulou, C., 2009). The number of nonlinear devices integrated with multilayer RAs warrants IM and EVM measurements to precisely determine the impacts of an RA on them. To that end, this work places a significant focus on characterizing the IM and EVM performance of the proposed RA.

The main contributions of this work, compared to similar works, can be summarized as follows:

1. Concurrent configuration of impedance bandwidth and radiation pattern.
2. High average realized gain (~9 dB) for all modes of operation in a relatively compact profile.
3. System-level performance investigation of the RA in terms of EVM and PIM.

Antenna Structure and Working Mechanism

1 Geometry of the Reconfigurable Antenna (RA)

The geometry of the RA, as shown in Figure (1), consists of four main layers, namely the feed layer, driven antenna (aperture-coupled patch), parasitic patch, and parasitic pixel layers. The aperture-coupled patch, which has been described in various works (Pozar, D.M., 1985), has been chosen for its relatively broad bandwidth and high degree of freedom in impedance tuning. The driven antenna couples electromagnetic (EM) energy to the parasitic patch and pixel layers, which are positioned 6.096 mm and 8.145 mm above the driven patch layer, respectively. These layers are formed using 1.52 mm and 0.813 mm thick RO400C substrates. Both layers are supported by four posts, with the air layers underneath serving as the primary low-loss medium see Figure (1).

The upper surfaces of the parasitic patch and pixel layers consist of grids of 3×3 and 3×2 metallic pixels, respectively. Adjacent rectangular metallic pixels in both parasitic patch and pixel layers are connected via PIN diode switches, as illustrated in the magnified sections of Figure (1a). A single PIN diode is also inserted into the microstrip feed line, as shown in the feed layer of Figure (1a), enabling changes to the length of the microstrip line, thereby achieving impedance matching. These PIN diodes are activated by applying a DC signal of 10 mA and 1.5 V to enable bandwidth and pattern reconfigurability. The typical activation mechanism of the PIN diodes has been detailed in our previous works (Rodrigo, D., Romeu, J., Cetiner, B.A. & Jofre, L., 2016).

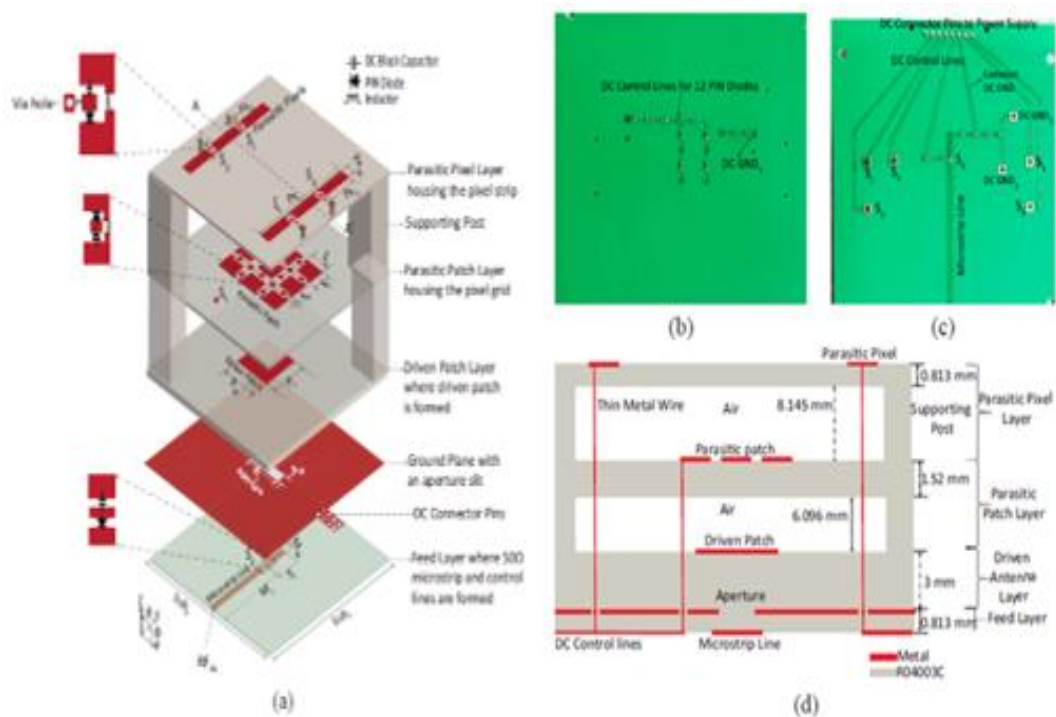


Figure 1): (a) 3D Exploded View of the RA; Photographs of the Bottom Face of the (b) Parasitic Patch Layer and (c) Feed Layer; and (d) AA' Plane Cross-Section of the RA.

As shown in Figure (1b), the DC controls for the 12 PIN diodes, which are required to interconnect the pixels in the parasitic patch layer, have been distributed from a single DC control line to reduce complexity. The DC control lines are formed on the bottom surface of the feed layer underneath the ground plane see Figure (1c). This structure provides shielding between control lines and radiating components, thereby minimizing the EM coupling between them, which in turn eliminates RF losses. Thin metal wires running through all the layers, as shown in Figure (1d), have been used to connect the DC control lines to the PIN diodes on the top surfaces of the parasitic patch and pixel layers.

An electromagnetic (EM) full-wave analysis tool was used to determine the geometrical dimensions of the overall structure and surface-mount device (SMD) component values, resulting in the desired impedance bandwidth variability and beam steering capabilities. The critical design parameters and manufacturer details of the SMD components are provided in Tables (1) and (2).

Table (1): Critical Design Parameters (in mm).

S_x, S_y	(6.4,6.4)	Sub_x, Sub_y	(90,90)	P_w, P_L	(18,18)
P_{xw}	3	M_w	1.82	M_L	52.85
S_L	8.65	S_D	1	P_{xL}	48
A_L, A_w	(16,0.8)	P_{xs}	15	P_{xG}	1.5

Table (2): Lumped Component Values and Self-Resonant Frequencies (SRF) Used in RA.

Component Type	Model	Value	SRF
PIN Diode	MA4AGFCP910	N/A	N/A
RF Choke	0603HP-39NXJLU	39 nH	3.5GHz
DC grounding inductor	0402HP-12NXGLU	12 nH	3.5GHz
DC block capacitor	GJM1555C1H1R3BB01D	1.3 pF	N/A
Bipolar Junction Transistor (BJT)	2N3904	N/A	N/A
Resistor (R1)	N/A	9.83 K Ω	N/A
Resistor (R2)	N/A	50.7 K Ω	N/A
Resistor (R3)	N/A	38 Ω	N/A

2 Working Mechanism

Bandwidth reconfigurability in the presented RA is achieved using the multiple resonance technique (Hall, P. & Schaubert, D., 1979). A driven patch is mutually coupled to a slightly larger parasitic patch (parasitic patch layer), which is pixelated into a grid of 3×3 metallic pixels. The effective electrical size of the parasitic patch can be increased or decreased by turning the interconnecting PIN diodes ON or OFF. Turning all the switches ON results in broad bandwidth operation, while keeping all the switches in the OFF state results in narrow bandwidth operation. Input impedance matching for broad and narrow bandwidth operations is accomplished by turning OFF and ON a single switch on the microstrip feed line, respectively.

The parasitic layer, housing two pixel strips, is placed 0.16λ (at 3.5 GHz) above the driven antenna layer. Beam steering is achieved by coupling EM energy from the driven and parasitic patch layers to the parasitic pixel layer. The Yagi-Uda principle can be used to explain the beam-steering property of this RA. The reconfigurable pixel strips act as reflectors or directors when their effective electrical lengths are changed by turning the interconnecting PIN diodes ON or OFF, enabling beam steering.

The switch statuses for achieving the desired bandwidth and beam-steering modes are provided in Table (3).

Table (3): Switch Configurations for Desired Modes of Operation (1 = ON, 0 = OFF, BW= Bandwidth, (θ , ϕ) indicate peak gain direction).

Modes	θ	ϕ	BW(MHz)	S1	S2	S3	S4	S5	S6
1	0^0	0^0	200	0	0	0	0	0	1
2	30^0	0^0	200	0	0	1	1	0	1
3	-30^0	0^0	200	1	1	0	0	0	1
4	0^0	0^0	800	0	0	0	0	1	0
5	30^0	0^0	800	0	0	1	1	1	0
6	-30^0	0^0	800	1	1	0	0	1	0

Measurement and Simulation Results

1 Impedance and Pattern Characterization

A prototype RA was fabricated using standard printed circuit board fabrication processes and characterized to validate the simulation results. PIN diode switches are numbered in Figures. (1a) and (1c) as S_i ($i=1, \dots, 6$) to identify the switch status for each mode. The switch configuration and associated modes of operation are shown in Table (3). S_1, S_2, S_3, S_4 represent the switches integrated on the parasitic pixel layer. S_5, S_5 represents the twelve PIN diodes used in the parasitic patch layer, as these switches are either all in the ON or all in the OFF states. S_6 is the switch integrated into the microstrip feed line. The maximum realized gain is approximately 8 dB for the broadside direction and approximately 9 dB for steered directions.

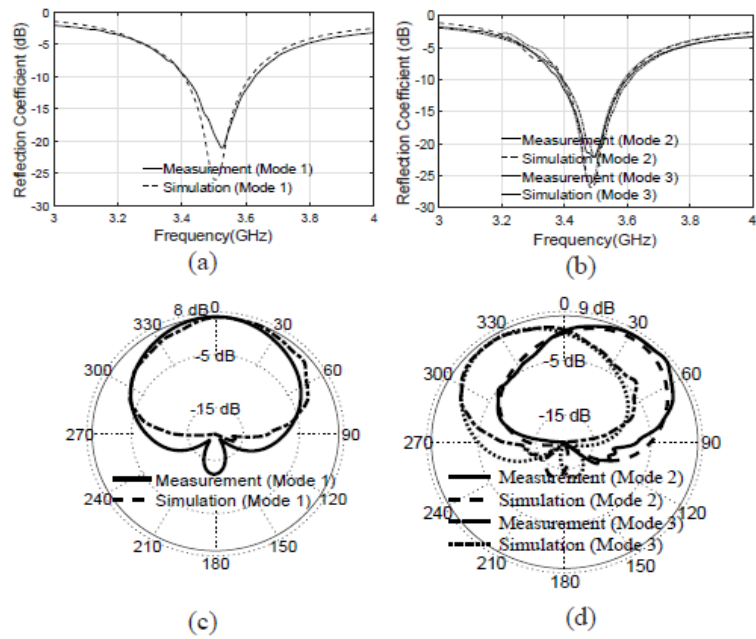


Figure (2): Simulated and Measured Reflection Coefficients of the RA for (a) Mode 1, (b) Modes 2 and 3, and Realized Gain Patterns for (c) Mode 1, and (d) Modes 2 and 3.

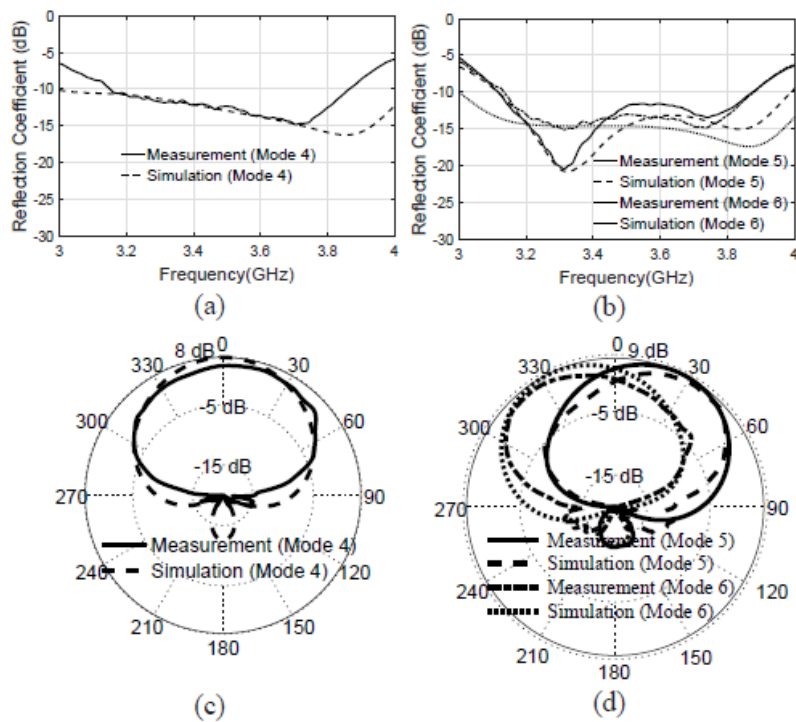


Figure (3): Simulated and Measured Reflection Coefficients of the RA for (a) Mode 4, (b) Modes 5 and 6, and Realized Gain Patterns for (c) Mode 4, and (d) Modes 5 and 6.

Conclusion and Future Works

A parasitic layer-based reconfigurable antenna (RA) targeting sub-6 GHz spectrum sharing applications, capable of dynamically changing its impedance bandwidths between narrow and broad frequency bands (3.4–3.6 GHz and 3.1–3.9 GHz) and concurrently steering its main radiation beam into three different directions (i.e., $\theta \in \{-30^\circ, 0^\circ, 30^\circ\}$ for $\phi \in \{0^\circ\}$), has been designed, manufactured, and characterized. Reflection coefficient and radiation pattern results obtained from measurements agreed well with the simulated results, indicating an average maximum gain of approximately 9 dB for all modes of operation.

As RA technology starts finding practical applications in today's and future transceiver systems, such as fifth-generation (5G) New Radio, the characterization of RAs in terms of system-level parameters, such as error vector magnitude (EVM) and passive intermodulation product (PIM), becomes important. The use of RF PIN diode switches in the presented RA causes minor degradation in EVM performance compared to passive horn antennas. For all six modes of operation, the EVM performance was satisfactory, with measured EVM values remaining below -25 dBm for an input power of 30 dBm.

References

- Ge, L. & Luk, K.M., 2016. Band-reconfigurable unidirectional antenna: A simple, efficient magneto-electric antenna for cognitive radio applications. *IEEE Antennas and Propagation Magazine*, 58(2), pp.18–27.
- Bhattarai, S., Park, J.-M.J., Gao, B., Bian, K. & Lehr, W., 2016. An overview of dynamic spectrum sharing: Ongoing initiatives, challenges, and a roadmap for future research. *IEEE Transactions on Cognitive Communications and Networking*, 2(2), pp.110–128.
- Hu, F., Chen, B. & Zhu, K., 2018. Full spectrum sharing in cognitive radio networks toward 5G: A survey. *IEEE Access*, PP, No. 99, pp.1–1.
- Chacko, B.P., Augustin, G. & Denidni, T.A., 2015. Electronically reconfigurable uniplanar antenna with polarization diversity for cognitive radio applications. *IEEE Antennas and Wireless Propagation Letters*, 14, pp.213–216.
- Goldsmith, A., Jafar, S.A., Maric, I. & Srinivasa, S., 2009. Breaking spectrum gridlock with cognitive radios: An information theoretic perspective. *Proceedings of the IEEE*, 97(5), pp.894–914.

- Tawk, Y., Costantine, J. & Christodoulou, C., 2014. Cognitive-radio and antenna functionalities: A tutorial [wireless corner]. *IEEE Antennas and Propagation Magazine*, 56(1), pp.231–243.
- Caromi, R., Xin, Y. & Lai, L., 2013. Fast multiband spectrum scanning for cognitive radio systems. *IEEE Transactions on Communications*, 61(1), pp.63–75.
- Erfani, E., Nourinia, J., Ghobadi, C., Niropo-Jazi, M. & Denidni, T.A., 2012. Design and implementation of an integrated UWB/reconfigurable-slot antenna for cognitive radio applications. *IEEE Antennas and Wireless Propagation Letters*, 11, pp.77–80.
- Ebrahimi, E., Kelly, J.R. & Hall, P.S., 2011. Integrated wide-narrowband antenna for multi-standard radio. *IEEE Transactions on Antennas and Propagation*, 59(7), pp.2628–2635.
- Tawk, Y. & Christodoulou, C., 2009. A new reconfigurable antenna design for cognitive radio. *IEEE Antennas and Wireless Propagation Letters*, 8, pp.1378–1381.
- Liu, Z., Boyle, K., Krogerus, J., de Jongh, M., Reimann, K., Kaunisto, R. & Ollikainen, J., 2009. MEMS-switched, frequency-tunable hybrid slot/PIFA antenna. *IEEE Antennas and Wireless Propagation Letters*, 8, pp.311–314.
- Hamid, M., Gardner, P., Hall, P.S. & Ghanem, F., 2011. Switched-band Vivaldi antenna. *IEEE Transactions on Antennas and Propagation*, 59(5), pp.1472–1480.
- Cetiner, B., Jafarkhani, H., Qian, J.-Y., Yoo, H.J., Grau, A. & De Fla-Viis, F., 2004. Multifunctional reconfigurable MEMS integrated antennas for adaptive MIMO systems. *IEEE Communications Magazine*, 42(12), pp.62–70.
- Miranda, F.A., Mueller, C.H. & Meador, M.A.B., 2014. Aerogel antennas communications study using error vector magnitude measurements. In: 2014 IEEE Antennas and Propagation Society International Symposium (APSURSI), July 2014, pp.1149–1150.
- Huff, G.H., Soldner, N., Palmer, W.D. & Bernhard, J.T., 2006. Study of error vector magnitude patterns (EVRP) for a transmit/receive pair of microstrip patch antennas. In: 2006 IEEE Antennas and Propagation Society International Symposium, July 2006, pp.449–452.
- Wilkerson, J.R., Kilgore, I.M., Gard, K.G. & Steer, M.B., 2015. Passive intermodulation distortion in antennas. *IEEE Transactions on Antennas and Propagation*, 63(2), pp.474–482.
- Wu, D., Xie, Y., Kuang, Y. & Niu, L., 2017. Prediction of passive intermodulation on mesh reflector antenna using collaborative simulation: Multi-scale equivalent method

and nonlinear model. *IEEE Transactions on Antennas and Propagation*, PP, No. 99, pp.1–1.

- Pozar, D.M., 1985. Microstrip antenna aperture-coupled to a microstripline. *Electronics Letters*, 21(2), pp.49–50.
- Sullivan, P. & Schaubert, D., 1986. Analysis of an aperture coupled microstrip antenna. *IEEE Transactions on Antennas and Propagation*, 34(8), pp.977–984.
- Li, Z., Ahmed, E., Eltawil, A.M. & Cetiner, B.A., 2015. A beam-steering reconfigurable antenna for WLAN applications. *IEEE Transactions on Antennas and Propagation*, 63(1), pp.24–32.
- Rodrigo, D., Romeu, J., Cetiner, B.A. & Jofre, L., 2016. Pixel reconfigurable antennas: Towards low-complexity full reconfiguration. In: 2016 10th European Conference on Antennas and Propagation (EuCAP), April 2016, pp.1–5.
- Ansoft Corp., 2015. HFSS. Pittsburgh, PA.
- Hall, P. & Schaubert, D., 1979. Wide bandwidth microstrip antennas for circuit integration. *Electronics Letters*, 15(15), pp.458–460.
- Zurcher, J.-F., 1988. The SSFIP: A global concept for high-performance broadband planar antennas. *Electronics Letters*, 24(23), pp.1433–1435.
- Croq, F. & Pozar, D.M., 1991. Millimeter-wave design of wide-band aperture-coupled stacked microstrip antennas. *IEEE Transactions on Antennas and Propagation*, 39(12), pp.1770–1776.
- Yuan, X., Li, Z., Rodrigo, D., Mopidevi, H.S., Kaynar, O., Jofre, L. & Cetiner, B.A., 2012. A parasitic layer-based reconfigurable antenna design by multi-objective optimization. *IEEE Transactions on Antennas and Propagation*, 60(6), pp.2690–2701.
- Rodrigo, D., Cetiner, B.A. & Jofre, L., 2014. Frequency, radiation pattern and polarization reconfigurable antenna using a parasitic pixel layer. *IEEE Transactions on Antennas and Propagation*, 62(6), pp.3422–3427.
- Uda, S., 1926. Wireless beam of short electric waves. *J. IEE*, pp.273–282.
- Yagi, H., 1928. Beam transmission of ultra short waves. *Proceedings of the Institute of Radio Engineers*, 16(6), pp.715–740.
- Huang, J., 1989. Planar microstrip Yagi array antenna. In: *Antennas and Propagation Society International Symposium, AP-S. Digest. IEEE*.

- Rodrigo, D., Jofre, L. & Cetiner, B.A., 2012. Circular beam-steering reconfigurable antenna with liquid metal parasitics. *IEEE Transactions on Antennas and Propagation*, 60(4), pp.1796–1802.